PASSOS: Passive Approximation Through Sum-of-Squares Orthogonal Rational Functions

Francisco Coronado [iD] and Arif Ege Engin [iD], *Member, IEEE*

Abstract—Signal and power integrity design in the time domain requires equivalent circuit models for interconnects and packages, whose descriptions may only be available as tabulated impedance or admittance parameters. Accurate models for these components should maintain their physical properties including causality, stability, and passivity. Sum-of-squares (SOS) polynomials, which are guaranteed to be non-negative, can be used to address the problem of generating passive scalar models, such as driving point impedances or admittances, based on an existing causal, stable, but nonpassive model. However, the poor conditioning of a monomial basis in SOS constraints prevents large-order modeling. In this article, we expand the SOS framework to reciprocal multiport admittance or impedance network parameters by introducing a methodology based on SOS matrices. In addition, orthogonalized rational functions are incorporated to solve the conditioning problem by embedding the denominator polynomial in the basis.

Index Terms—Macromodeling, passivity, rational function, sum-of-squares (SOS), stability, transfer function, vector fitting.

I. INTRODUCTION

MACROMODELING of passive networks for signal and power integrity design is critical for accurate time domain simulation. Several rational function fitting techniques exist to produce guaranteed stable and causal models, such as the widely popular vector fitting algorithm [1] as well as versions of AAA and the Loewner matrix methods with stable poles [2], [3]. These methods provide accurate models with stable poles, however, passivity conditions are not enforced. A nonpassive rational function approximation may describe a system that produces energy at particular frequency ranges which can lead to unintended consequences if not accounted for.

Techniques to enforce passivity are typically implemented as a postprocessing measure from an already causal and stable system. A closed form of the bounded-real/Kalman–Yakubovich–Popov (KYP) lemma conditions is used in [4] to exploit only the nonpassive components of a partially passive or causal and stable state-space model . Skew-Hamiltonian/Hamiltonian matrix pencils are implemented in [5] in an adaptive sampling approach to identify violations followed by a passivity loop for corrections. The residue perturbation scheme of [6] aims to improve on similarly existing techniques by refining the perturbation of the residues with a scaling factor based on the relationship between the perturbation of the half-size singular test matrix and eigenvalue perturbation. A parameterized version of bounded real lemma conditions is used in [7], based on reformulations of the residue and direct terms as sums of the Bernstein polynomials which are known to be non-negative. The iterative Loewner matrix-based method [8] introduces additional data points until a passive model is obtained followed by a spectral zeros method. The equivalence of passivity conditions or KYP lemma to sum-of-squares (SOS) polynomials has been shown [9], [10], [11]. However, a recent survey of passivity enforcement techniques [12] does not include any SOS-based algorithm.

For passive admittance or impedance parameters, a fundamental requirement is that the real part of the transfer function must be non-negative for all real frequency intervals. Assuming an existing stable but nonpassive model, the real part of the rational function consists of a non-negative denominator polynomial. Univariate non-negative polynomials are known to have an SOS decomposition, thus, the goal is to fit an SOS polynomial to the numerator. We used a Chebyshev basis in [13] and an orthogonal rational basis in [14] to improve the numerical stability in generating passive models for one-port networks.

In this article, we present a method to generate passive models for multiport networks using SOS orthogonal rational matrices (PASSOS). A very critical consideration for large-order passive approximation is the numerical conditioning. Use of a perfectly conditioned orthogonal polynomial basis (such as Chebyshev polynomials) still suffers from ill-conditioning due to the division by the denominator polynomial in a rational function. We overcome this source of ill-conditioning by generating an orthogonal rational basis directly through an Arnoldi iteration, thereby integrating the prescribed denominator in the basis. We present a passivity test for strictly proper transfer functions based on a state-space representation of such orthogonal rational functions to confirm the results. Numerical results from examples of a common-mode filter, a stripline, and power/ground planes demonstrate the accuracy and efficiency of this approach.

II. SYMMETRIC PASSIVE RATIONAL FUNCTIONS

Assume that a transfer function matrix representing impedance or admittance parameters is given as a rational

function or in pole-residue form as

$$R(s) = \frac{F(s)}{a(s)} = \frac{\sum_{i=0}^{m} F_i s^i}{\sum_{i=0}^{n} a_i s^i} = D + sK_0 + \sum_{i=1}^{n} \frac{K_i}{s - p_i} \quad (1)$$

where we assume that the network is reciprocal and represented by a common set of poles p_i. The coefficients F_i are matrices and a_i are scalars. This rational matrix will be passive, or equivalently positive real, if it satisfies the following conditions [15].
1) The coefficients F_i, a_i are real (i.e., $R^*(s) = R(s^*)$).
2) All poles p_i are stable, that is they do not have positive real parts. If there are any pure imaginary poles, they should be simple and have positive semidefinite (PSD) residue matrices.
3) The real part of the rational function is PSD at all real frequencies ω, i.e., $\text{Re}(R(j\omega))$ has non-negative eigenvalues or $\text{Re}(R(j\omega)) \geq 0$.

The first two conditions can be enforced by using real arithmetic in fitting the coefficients and flipping the signs of unstable poles [1], [2], [3]. The second condition limits the degree of the polynomials such that $|n - m| \leq 1$ as pure imaginary poles should be simple. In the following, we assume there are no pure imaginary poles and $m = n$ to simplify our presentation.

We can obtain the real part of $R(j\omega)$ as

$$\frac{F(j\omega)a^*(j\omega) + F^*(j\omega)a(j\omega)}{2a(j\omega)a^*(j\omega)} = \frac{N(\omega^2)}{|a(j\omega)|^2}. \quad (2)$$

The real part of a rational function will be an even function of frequency; hence the numerator polynomial N will be a function of ω^2. Assuming that $a(s)$ is known and has zeros on the left half plane only, $R(s)$ will represent a passive network if its real part given in (2) is PSD (i.e., $N(\omega^2) \geq 0$). Such a univariate matrix is PSD if and only if it is a sum-of-squares (SOS) polynomial matrix [16] given by

$$N(\omega^2) = M^T(\omega)M(\omega) \quad (3)$$

where the degree of each polynomial in matrix $M(\omega)$, which can be a rectangular matrix, is smaller than or equal to n. We will see that our numerical method is better conditioned when we include the denominator as

$$\frac{N(\omega^2)}{|a(j\omega)|^2} = \frac{M^T(\omega)}{|a(j\omega)|} \frac{M(\omega)}{|a(j\omega)|} \quad (4)$$

which we will call an SOS rational matrix.

The basis of our approach is to enforce the PSD constraint on the real part of the rational matrix using such SOS rational matrices. The approximation problem can then be expressed as a norm minimization problem with a PSD constraint given as

$$\text{minimize} \quad \sum_{i=1}^{l} ||R(j\omega_i) - H_i||_F^2$$

$$\text{subject to} \quad \frac{N(\omega^2)}{|a(j\omega)|^2} \geq 0 \quad (5)$$

where H_i is the provided impedance or admittance data at l frequency points, and we use the Frobenius norm.

The positive real lemma provides an alternative set of conditions for passivity based on a minimal state-space representation of the rational function $R(s) = C(sI - A)^{-1}B + D$. The third passivity condition can be replaced with the feasibility of the following linear matrix inequality:

$$\begin{bmatrix} A^T P + PA & PB - C^T \\ B^T P - C & -2D \end{bmatrix} \leq 0 \quad (6)$$

in the symmetric matrix variable P [17]. P will necessarily be a positive-definite matrix since the poles are stable.

III. SOS RATIONAL MATRICES

In [13], we enforce the non-negativity constraint for passive scalar functions by expressing the real part numerator as an equivalent SOS representation. We extend this methodology to multiport networks in this article. One way to test whether a univariate polynomial matrix $N(\omega^2)$ is PSD is through the Gram matrix P [16] of the SOS representation

$$N(\omega^2) = ([\omega] \otimes I)^T P([\omega] \otimes I), \quad P \geq 0 \quad (7)$$

where P is a symmetric PSD matrix, I is the identity matrix of size equal to the number of ports, and the monomial vector is given as $[\omega] = (1, \omega, \ldots, \omega^n)^T$. This allows us to solve the problem using a semidefinite program; a feasible solution for a PSD P proves that $N(\omega^2)$ is a PSD polynomial matrix. The semidefinite program searches for a PSD P subject to the equality constraints of the polynomial coefficients on both sides of (7).

A. Even Symmetry

Since $N(\omega^2)$ is an even function, we can reduce the problem size by exploiting the symmetry following [18] as

$$N(\omega^2) = E^T(\omega)E(\omega) + O^T(\omega)O(\omega) \quad (8)$$

where E and O are matrices of even and odd polynomials, respectively. The corresponding Gram matrix representations can be obtained as

$$E^T(\omega)E(\omega) = ([\omega_e] \otimes I)^T P_e([\omega_e] \otimes I), \quad P_e \geq 0$$

$$O^T(\omega)O(\omega) = ([\omega_o] \otimes I)^T P_o([\omega_o] \otimes I), \quad P_o \geq 0 \quad (9)$$

where the even and odd rational basis vectors are given as

$$[\omega_e] = (1, \omega^2, \ldots, \omega^n)^T \quad (10)$$

$$[\omega_o] = (\omega, \omega^3, \ldots, \omega^{n-1})^T \quad (11)$$

assuming n is even. For odd n, $[\omega_e] = (1, \omega^2, \ldots, \omega^{n-1})^T$, $[\omega_o] = (\omega, \omega^3, \ldots, \omega^n)^T$.

B. Sampling

The semidefinite program suffers from poor conditioning that involves the coefficients of a monomial basis in SOS constraints. One way to avoid working directly with the coefficients of polynomials is to make use of the property that an nth degree polynomial is uniquely defined by sampling it at least at $n + 1$

points [19], [20]. Accordingly, a sampling-based formulation of the SOS constraint in (5) can be given as

$$\text{Re}\,(R(j\omega_i))$$
$$= \frac{([e_i] \otimes I)^T P_e([e_i] \otimes I) + ([o_i] \otimes I)^T P_o([o_i] \otimes I)}{|a(j\omega_i)|^2}$$
$$i = 1, \ldots, l$$
$$P_e \geq 0, P_o \geq 0. \tag{12}$$

We can observe that the first line of (12) is equal to the real part of $R(j\omega)$ evaluated at the sampling point $\omega = \omega_i$. The right-hand side are the samples of a non-negative polynomial matrix of the same degree divided by the denominator polynomial. The monomial basis at the sampling points are given as $[e_i] = (1, \omega_i^2, \ldots, \omega_i^n)^T$, and $[o_i] = (\omega_i, \omega_i^3, \ldots, \omega_i^{n-1})^T$ for even n. There are two issues to be addressed at this point. First, the ill-conditioning due to the use of a monomial basis. Second, the division by $|a(j\omega_i)|^2$, as it can have a large variation over the frequency samples. Next we present an Arnoldi iteration [21] to generate orthogonal basis rational functions to solve both sources of ill-conditioning.

C. Orthogonal Rational Function Basis

Consider a rational function $r(\omega) = n(\omega)/|q(j\omega)|$, where the numerator polynomial is given in a monomial basis as $n(\omega) = \sum_{i=0}^{n} c_i \omega^i$ and the denominator is given in terms of its values at l frequency points as $d_i = 1/|q(j\omega_i)|$ and $d = (d_1, d_2, \ldots, d_l)^T$. The coefficients of $n(\omega)$ can be calculated from

$$D \begin{bmatrix} 1 & \omega_1^1 & \ldots & \omega_1^n \\ 1 & \omega_2^1 & \ldots & \omega_2^n \\ \vdots & \vdots & \ddots & \vdots \\ 1 & \omega_l^1 & \ldots & \omega_l^n \end{bmatrix} \begin{bmatrix} c_0 \\ c_1 \\ \vdots \\ c_n \end{bmatrix} \approx \begin{bmatrix} h_1 \\ h_2 \\ \vdots \\ h_l \end{bmatrix} \tag{13}$$

or $DVc \approx h$, where $D = \text{diag}(d)$, and h is the vector of the data at the given frequency points. It is well known that the Vandermonde matrix V becomes ill-conditioned for high orders of approximation n. To overcome this issue, an orthogonal polynomial basis at the given frequency points can be generated using an Arnoldi iteration to orthogonalize V. It has been shown that the multiplication with D can still deteriorate the numerical conditioning [21]. Instead, an orthogonal basis Q can be obtained for the whole rational function (or DV) by starting the Arnoldi iteration with d as the initial vector. We choose the norm of each column to be $\sqrt{l}$. Hence, the rational approximation problem can be expressed as

$$Qf \approx h \tag{14}$$

where f are the coefficients of the orthogonal rational function. The monomial basis used in (12) can be obtained from row i of V as $[e_i] = (v_{i0}, v_{i2}, \ldots, v_{in})^T$, and $[o_i] = (v_{i1}, v_{i3}, \ldots, v_{i(n-1)})^T$. We simply replace them with rows of Q for representation in an orthogonal rational basis (which also

includes the contribution of $|a(j\omega_i)|$) as

$$\text{Re}\,(R(j\omega_i))$$
$$= ([E_i] \otimes I)^T U_e([E_i] \otimes I) + ([O_i] \otimes I)^T U_o([O_i] \otimes I)$$
$$i \in \{1, \ldots, l\}$$
$$U_e \geq 0, U_o \geq 0 \tag{15}$$

where

$$[E_i] = (q_{i0}, q_{i2}, \ldots, q_{in})^T$$
$$[O_i] = (q_{i1}, q_{i3}, \ldots, q_{i(n-1)})^T \tag{16}$$

for even n. Sampling should be done at least at a subset of $n + 1$ frequency points from the given data set. However, sampling at more frequency points is possible and can have an impact on the conditioning of the problem. In this article we sample at approximately $2n$ points (assuming $2n \leq l$), by skipping over the frequency points appropriately to cover the whole range of frequencies. In order to ensure the orthogonal basis in (16) maintains the even–odd symmetry, we include the negatives of the frequency points as well in generating the orthogonal basis Q. Note that (13) includes a right-hand side of data samples h for illustration purposes only. The generated basis Q is independent of this right-hand side and solely depends on the starting vector d and frequency samples ω. As a result, the same basis Q would be used for all the elements of a multiport network matrix as well.

We have the flexibility to have a different basis on both sides of the equation on the first line of (15) as the equality is in terms of the values and not coefficients. The right-hand side are the samples of a non-negative even rational function expressed in an orthogonal basis for good numerical conditioning. The left-hand side can for example be expressed in a partial fractions basis, such as used in vector fitting [1], or in barycentric form, as in AAA [2], [22]. In the following we use an orthogonal basis for the left-hand side as well, based on the Arnoldi iteration [21].

IV. STATE-SPACE MODEL FOR ORTHOGONAL RATIONAL FUNCTIONS

One way to export the model in a standard format is to generate a state-space model. This allows the model to be used in simulators and verify whether the model is indeed passive. To that purpose, it is possible to represent the rational function in (1) using an orthogonal basis [23] as well to yield

$$R(s) = \frac{\sum_{i=0}^{m} F_i s^i}{\sum_{i=0}^{n} a_i s^i} = \frac{\sum_{i=0}^{m} G_i u_i(s)}{\sum_{i=0}^{n} b_i u_i(s)} \tag{17}$$

where we assume that the denominator polynomial coefficients a are known and an orthogonal basis u is obtained based on the samples of this denominator and the frequency points. Therefore, u already includes the division by the denominator similar to (14), and G would be the only free variables in the optimization problem of (5) to represent the rational function $R(s)$ in an orthogonal basis. This would be sufficient for approximation or interpolation purposes; however, a rational function is needed

---

Algorithm 1: Algorithm for Passive Modeling of Multiport Networks using SOS Orthogonal Rational Matrices (PAS-SOS).

Input: Strictly stable denominator $a(j\omega_i)$, data Y_i at l frequency points ω_i; order n
Output: State-space model (A, B, C, D) of a passive rational function
1: $d \leftarrow 1/a$
2: $d \leftarrow d\sqrt{l}/\text{norm}(d)$
3: $Q \leftarrow$ Arnoldi basis starting with $|d|$
4: $E_i, O_i \leftarrow$ slices of Q following (16)
5: $U, H \leftarrow$ Arnoldi basis starting with d
6: $G \leftarrow$
    minimize $\sum_{i=1}^{l} ||\sum_{k=0}^{n} G_k u_{ik} - Y_i||_F^2$ s.t. (15)
7: $b \leftarrow$ minimize $\sum_{i=1}^{l} |\sum_{k=0}^{n} b_k u_{ik} - 1|^2$
8: $A, B, C, D \leftarrow$ state-space from H, G, b following (18)

---

for representation in state-space form. This is achieved by using the same orthogonal basis u, and finding the coefficients b of the denominator such that $\sum_{i=0}^{n} b_i u_i(s) = 1$. This is solved as a least squares problem; however, the results will be precise as we are fitting data obtained from a same-order polynomial. So the problem we are solving is equivalent to calculating the coefficients of $b(s)$ from $b(s)/a(s) = 1$, given $a(s_i), i = 1, \ldots, l$ and $l \geq n + 1$. We have a solution if the degrees of $b(s)$ and $a(s)$ are the same, and $b(s)/a(s) = 1$ holds at every point.

It is useful to note that we do not need an explicit representation of the orthogonal basis polynomials $u_i(s)$ to use them in the optimization problem (5). All that is needed is their evaluation at discrete frequency points that is already available as $u_i(s_k) = u_{ki}$, where u_{ki} are the elements of an $l \times (n+1)$ matrix U with orthogonal columns obtained through the Arnoldi iteration. The Arnoldi iteration also provides an $(n + 1) \times n$ upper Hessenberg matrix H. To integrate such a model in circuit simulators, or to test for passivity, a state-space representation can be used. For the case $(m < n)$, a state-space transformation is given in [23], which can be extended for the $(m = n)$ case as

$$A = H_n^T \otimes I - h_{n+1,n}(e \otimes I)(b_{0:n-1}^T/b_n \otimes I)$$
$$B = h_{n+1,n}(e \otimes I)/b_n$$
$$C = (G_0 \ G_1 \ \ldots \ G_{n-1}) - (b_{0:n-1}^T/b_n \otimes G_n)$$
$$D = G_n/b_n \tag{18}$$

where H_n is an $n \times n$ matrix obtained from H by removing its last row, $h_{n+1,n}$ is the bottom-right element of H, $b_{0:n-1}$ is the denominator coefficient vector except for the last element, e is a vector of $n - 1$ zeros followed by a 1 as its last element, I is the identity matrix of dimensions equal to the number of ports, and $\otimes$ represents the Kronecker product.

The overall PASSOS algorithm including the generation of such a state-space model is summarized in Algorithm 1.

This specific state-space representation is one possible realization. A simpler approach would be to fit the residues to the passive model approximation obtained in Step 6 of the algorithm.

As the order of the models match, we would once again obtain a precise fitting of the residues with guaranteed passivity. This is related to the unique definition of an nth degree polynomial through its values at greater than n points. A more thorough description of the orthogonal rational approximation, along with a Matlab code to generate state-space models out of that are presented in [24].

V. TEST FOR PASSIVITY

The SOS formulation or the positive real lemma allows us to solve the passive approximation problem. They could also be solved for feasibility, in order to test whether a given rational function is passive. For this latter case, a numerically more efficient approach is through the test matrix S obtained from a state-space representation by

$$S = A(BD^{-1}C - A). \tag{19}$$

S should have no positive-real eigenvalues. If it does, then the square-root of the positive-real eigenvalues are the frequencies where passivity violations start or end [25]. In the following, we extend this test when there is no D term.

The passivity test above requires that the matrix D is nonsingular, otherwise a transformation of variables is needed [26]. A common case is a strictly proper transfer function with no D term, which occurs when $m = n - 1$ in (1). In general, the real and imaginary parts of a transfer function can be separated [27], [28], [29] using

$$(j\omega I - A)^{-1} = -A \left(\omega^2 I + A^2\right)^{-1} - j\omega \left(\omega^2 I + A^2\right)^{-1} \tag{20}$$

to yield

$$\text{Re}(R(j\omega)) = -C \left(\omega^2 I + A^2\right)^{-1} AB \tag{21}$$

which is a strictly proper transfer function in the variable ω^2. Its zeros would be the same as the zeros of

$$\omega^2 \text{Re}(R(j\omega)) = CA^2 \left(\omega^2 I + A^2\right)^{-1} AB - \mathbf{CAB} \tag{22}$$

after discarding the zeros introduced at 0. At the zeros of this transfer function, $N(\omega^2)$ becomes singular, indicating frequency points where passivity violations begin or end. The zeros of $\text{Re}(\omega^2 R(j\omega))$ can be obtained from the eigenvalues of its inverse state-space matrix

$$T = -A \left(I^2 + B(\mathbf{CAB})^{-1}CA\right) A. \tag{23}$$

This test applies only to symmetric network functions similar to (19) [28]. To summarize, the eigenvalues of the test matrices S and T can be used to detect possible passivity violations of a transfer function with and without a D matrix, respectively.

VI. NUMERICAL RESULTS

In this section, we provide several numerical examples of simulated and measured admittance or impedance data. The eigenvalues of the real part transfer function approximations are plotted for the approximated stable and passive models. Eigenvalues of the test matrices described earlier are also shown with asterisks (denoted as passivity violations in the figures)

to show frequency ranges for nonpassive behavior of stable models. In addition, plots of the passive magnitude transfer function approximation are provided alongside the original data. Eigenvalue and magnitude plots display the upper triangular portions of the approximated symmetrical data. In all examples, SOS models correctly enforced passivity. All algorithms are running on a computer using Windows 11 with an 11th Gen Intel(R) Core(TM) i7-11700 K 3.60 GHz eight core CPU.

The first example is a pair of solid power/ground planes that have been simulated at 301 frequencies using the finite difference method [30] to obtain admittance parameters of two symmetrical ports. This example is chosen as simulation or measurement errors may result in nonpassive initial data in practical examples. The eigenvalues of the real part admittance data indicate nonpassive behavior in three frequency ranges near the center of the frequency range. Vector fitting was used to obtain a model with 40 stable poles after 20 iterations. The result was an excellent match to the eigenvalues of the provided data; therefore the outcome was also a nonpassive model. Fig. 1 shows the comparison of the passive and nonpassive eigenvalues of the rational functions with the provided data. In Fig. 1(b), the SOS model follows the behavior of the stable model while maintaining non-negativity within the nonpassive region of the stable model. The magnitude plot in Fig. 1(c) shows the SOS approximation agreeing well with the original data.

The second example is from a two-port stripline measured at 5001 frequencies with data approximated using 40 poles and 20 iterations of vector fitting. Fig. 2(a) indicates eight frequency bands of passivity violations in the stable model. An example frequency band is shown in Fig. 2(b) with two passivity violations with a center frequency of 78 GHz. The eigenvalues of the real part of the passive model identified and corrected all violations while maintaining a low rms error of 9.60E-03 in comparison to 9.56E-03 of vector fitting. The SOS model maintains a good fit to this larger dataset, as seen in the magnitude plot, Fig. 2(c).

The third example is a four-port common-mode filter for differential lines [31]. The measurement is done with a vector network analyzer across 1001 frequencies to obtain the admittance parameter data of its four ports. The stable model is obtained through vector fitting using 50 poles and 20 iterations. Fig. 3 shows the comparison of the nonpassive model with 50 poles against passive models having the same number of poles from SOS, residue perturbation through the Matrix Fitting Toolbox (MF) [32], and KYP lemma (KYP) approaches. The nonpassive model has an rms error of 1.98E-03, however, results in many frequency bands with passivity violations. Enforcing passivity with an SOS approach leads to a model with slight increase in error of 2.41E-03. Two of the passivity violations occurring in the admittance parameters of the stable model are shown in the frequency range near 38.2 GHz provided in Fig. 3(b). The SOS approximation results in a model with eigenvalues touching zero but not crossing, while also preserving the vector fitting behavior. Observing the magnitude plot in Fig. 3(c), SOS using orthogonal rational functions continues to provide good fits with increasing ports size. In this example, the passivity test matrix of the model approximation based on the KYP lemma indicated very small passivity violations near the beginning of the dataset. Upon further inspection, there was no sign of a passivity
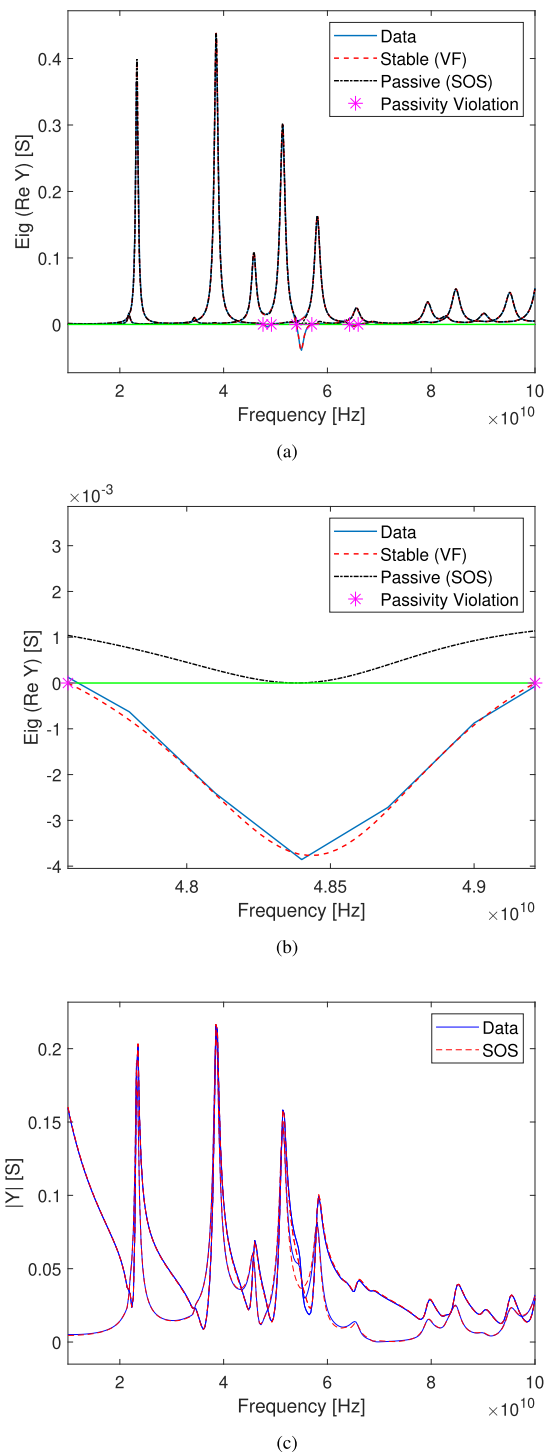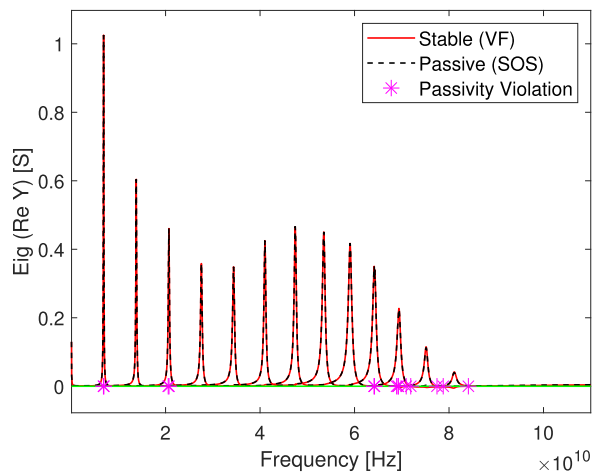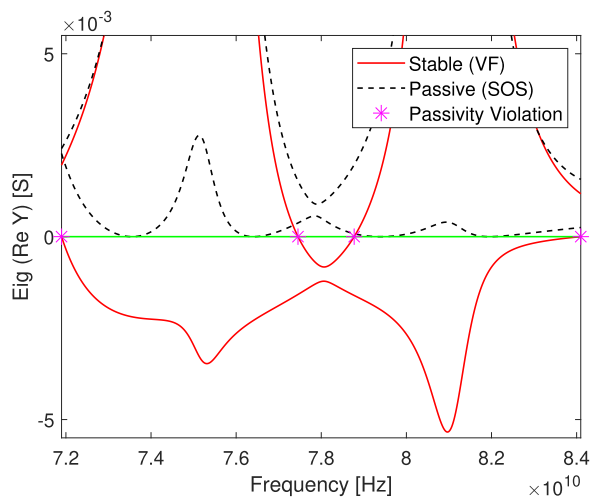

Fig. 1. (a) Full and (b) zoomed-in eigenvalue plots derived from the input admittance of a multiport simulation solid power/ground planes. The nonpassive model resulted in three frequency bands with passivity violations as shown. (c) Magnitude of the passive admittance parameters alongside the original data.

violation through a sweep of the eigenvalues of the real part. This may be due to the sensitivity of the eigenvalue calculation of test matrices in the case of closely spaced eigenvalues.
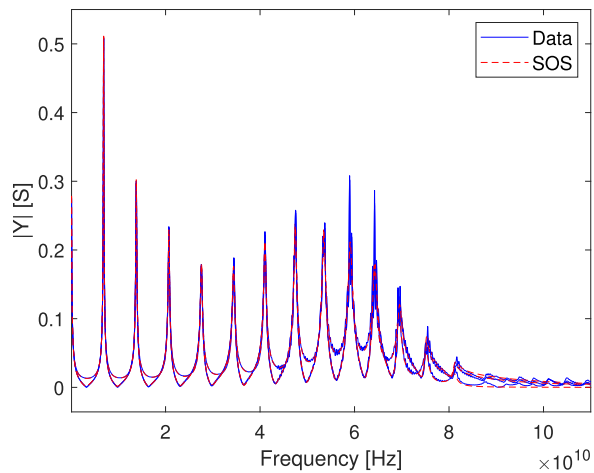
Timings and rms errors of different models are collected for various approximation orders in terms of the number of poles, as seen in Fig. 4. In Fig. 4(a), the rms error plot with respect to number of poles clearly shows the cost associated with enforcing
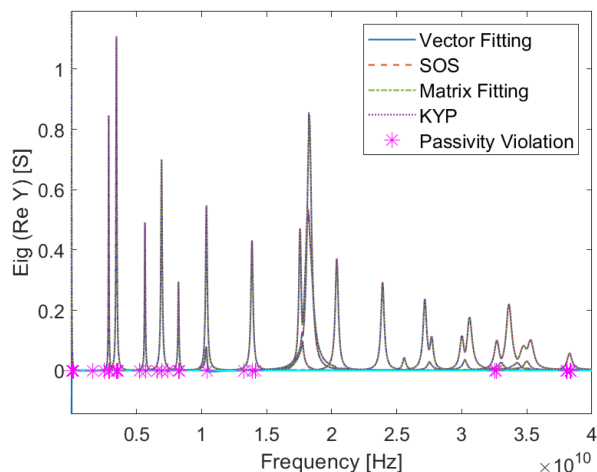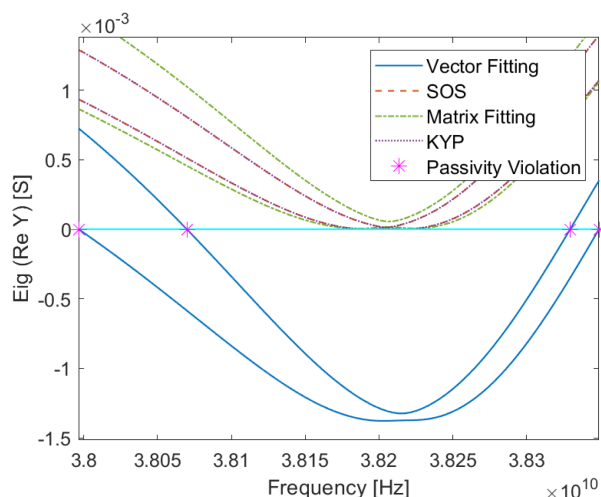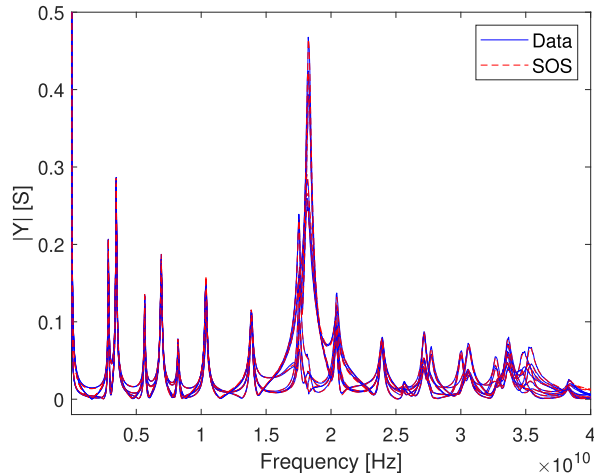
Fig. 2. (a) Full and (b) zoomed-in eigenvalue plots derived from the real part of the admittance parameters of a multiport stripline measurement. The nonpassive model resulted in eight frequency bands with passivity violations as shown. (c) Magnitude of the passive admittance parameters alongside the original data.

Fig. 3. (a) Full and (b) zoomed-in eigenvalue plot of the real part of admittance parameters of a four-port common-mode filter measurement. The nonpassive model results in many passivity violations as shown. In (c) the magnitude of the SOS approximation shows good agreement with the original data.

TABLE I
RMS Errors of Multiport Models

Example	Poles	VF	SOS	MF	KYP
1	2×40	1.58E-4	2.64E-03	2.80E-03	2.65E-03
2	2×40	9.56E-03	9.60E-03	9.61E-03	9.60E-03
3	4×50	1.98E-03	2.41E-03	2.56E-03	2.41E-03
4	10×50	8.50E-02	8.55E-02	8.65E-02	-

occurring in larger order models is expected and is due to the added complexity of the semidefinite problem.

The last example is of a ten-port cavity resonator from a simulation using the full-wave analysis tool, Sonnet [33]. The impedance parameters are collected over a range of 600 frequencies from 100 MHz to 60 GHz and are approximated using 50 stable poles with 20 iterations of vector fitting. The eigenvalues of the real part admittance of the stable model in Fig. 5(a) result in ten real roots in the region of 10–20 GHz. Fig. 5(b) shows one of the frequency bands, where a passivity violation occurs in the vector fitting model. Both SOS and MF passive solutions correct the violations with differing model behavior, as shown in the figure. Comparing to the original data, vector fitting approximates a stable model with an error of 8.50E-02; whereas, the corrections with SOS lead to an increased error of 8.55E-02. The magnitude of the passive SOS impedance parameters are overlaid on top of the corresponding data in Fig. 5(b). A model using the KYP lemma could not be obtained for this example as the memory resources were exceeded.

VII. RESULTS AND DISCUSSION

The multiport rms errors of the transfer functions and timings are collected and listed in the following tables. The errors are calculated with respect to the upper triangular portions of the symmetrical data in each example. The timings include only the passivity enforcement function calls and not the stable pole extraction time. In these tables, we have included results from existing approaches: residue perturbation through the Matrix Fitting Toolbox and the KYP lemma. The KYP lemma approach was implemented as a norm-minimization problem using the stable state-space model result from vector fitting according to (6). Both the KYP lemma and PASSOS formulated problems are solved using the CVX Package [34]. In order to produce viable results for these large orders with the KYP lemma, both frequency scaling and constraint scaling were used. In the tables, vector fitting and Matrix Fitting Toolbox results are denoted by the abbreviations VF and MF, respectively.

Considering the rms errors in Table I, the stable results from vector fitting provide an accurate fit to the data as expected while the passive approximation approaches are all on the same order of magnitude for each example. SOS provides the globally optimum fit for the numerator, as demonstrated by its equivalence to KYP results. The four examples correspond to Figs. 1, 2, 3, and 5, respectively. The first example demonstrates the tradeoff cost for a physical model as all passive approximations exhibit over an order of magnitude increase in error. This was anticipated for the first example since the data itself was nonpassive. In the second example, the accuracy of all passive results appears identical
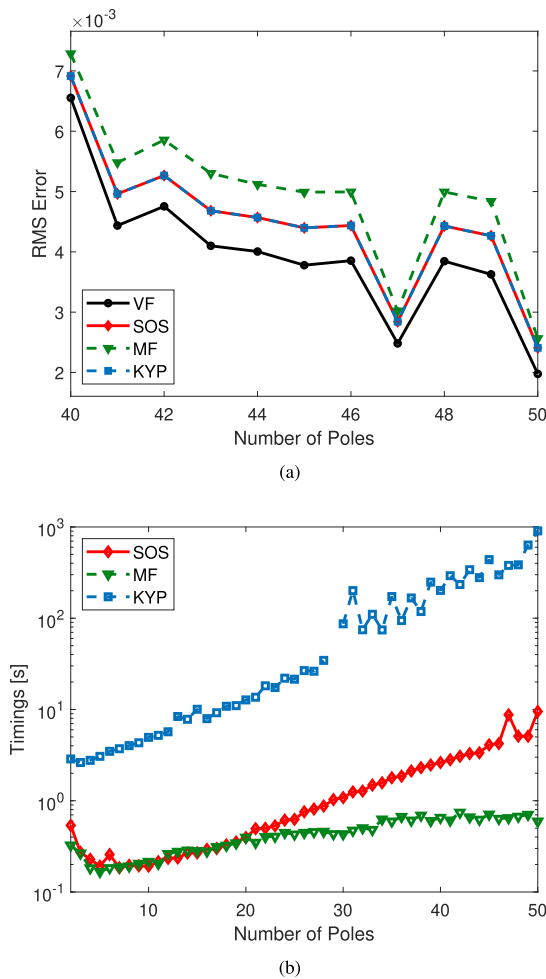
Fig. 4. Collected rms errors and timings using the common-mode admittance parameter data of example 3, for various approximation orders in the number of poles. (a) RMS errors of the stable VF model and passive SOS, KYP, and MF models from 40–50 poles. (c) Timings of the three passivity enforcement algorithms with the KYP lemma failing to solve for a 29 pole solution. The SOS algorithm converges to an equivalent KYP solution in all comparable cases while maintaining roughly an order of magnitude difference in solving time.

passivity as SOS, MF, and KYP solutions deviate from the stable vector fitting results. The three distinct curves corresponding to the stable (VF), passive optimal (SOS and KYP), and passive suboptimal (MF) solutions. The SOS algorithm converges to the equivalent KYP solution at roughly an order of magnitude faster across the pole variation shown in the semilog plot Fig. 4(b). Notably, the KYP lemma fails to solve for a solution with 29 poles which is indicated by the gap in the KYP data of the same figure. We found that the direct application of KYP lemma was numerically unstable. We did two things to make it work for higher orders: 1) frequency normalization and 2) scaling the PSD matrices in the semidefinite program. Depending on the scaling factor, the semidefinite program had trouble converging. This numerical instability is a major handicap for the direct use of KYP lemma. We did not use any frequency or PSD matrix scaling in PASSOS.

For approximation orders up to 20 poles, SOS is able to produce solutions in comparable times to MF. The deviation
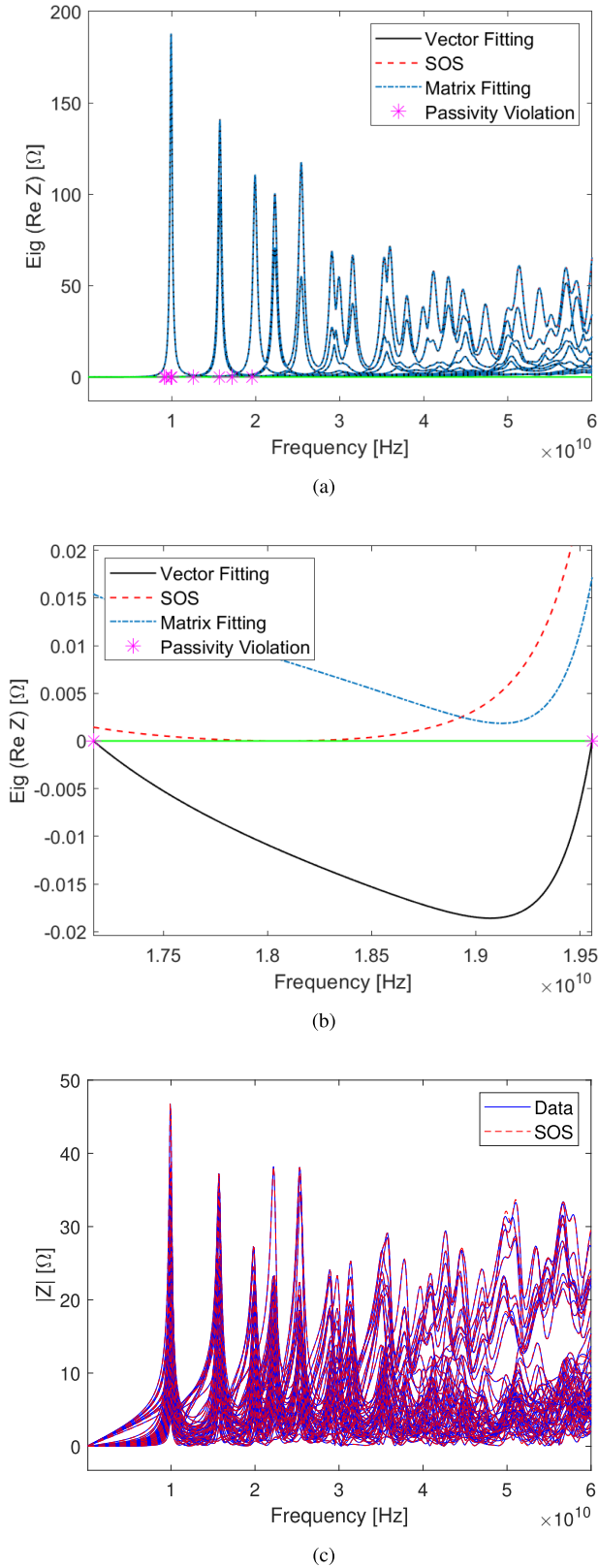
Fig. 5. (a)–(c) Model approximations using the impedance parameters of a simulated ten-port cavity resonator. (a) Eigenvalues of the real part impedance across the entire frequency range of data. (b) A frequency band showing passive approximations using an initial stable but nonpassive vector fitting model. (c) Magnitude plot including the original impedance parameter data and the passive SOS approximation.

TABLE II
TIMINGS OF PASSIVE MULTIPORT MODELS IN SECONDS

Example	Poles	SOS	MF	KYP
1	2×40	0.79	0.40	8.06
2	2×40	0.92	1.25	66.9
3	4×50	9.51	0.59	906
4	10×50	97.2	3.46	-

but, as seen in Fig. 3(b), there are two distinct solutions; the suboptimal and optimal solutions. A similar trend is observed in example 3, which doubles the port size from 2 to 4 and increases the approximation order to 50. Increasing the port size again to 10 ports, the high complexity of the LMI constraints in the KYP lemma becomes an issue and causes our system to exceed the available memory resources. As a result, a solution using the KYP lemma could not be obtained. The PASSOS framework is well conditioned and more efficient to enforce passivity of larger models and finds a solution with the lowest error. Next, observing the timings in Table II, the computational cost of KYP for high model order is visible across all examples. The LMIs of the KYP lemma require several seconds to minutes to reach a passive solution, whereas SOS and matrix fitting methods determine a passive model in a fraction of the time. For the larger 10 port example 4, as mentioned previously, a KYP lemma-based solution for 50 poles cannot be solved; solving for a 20 pole solution requires over 930 s or 15.5 min. The equivalent SOS-based algorithm significantly lowers the solving time and allows for a globally optimal passive approximation. Timings for SOS in the first two examples, with two ports, are comparable in order to passivity enforcement with matrix fitting. The residue-perturbation-based approach outperforms SOS timings in examples 1, 3, and 4, however, falls behind for example 2. For passivity assessment, the Matrix Fitting Toolbox is known to establish an assortment of frequency points with passivity violations. Therefore, the example 2 timings may likely be contributed to the larger size of 5001 frequency points in comparison to the 301 and 1001 points of the first and third examples, respectively. The difference in timings of the last example are related to the efficiency of the quadratic problem being solved with the residue perturbation approach.

VIII. CONCLUSION

In this article, we have introduced PASSOS for passive approximation using SOS orthogonal rational functions. Instead of using SOS polynomials to fit residues, we incorporated the denominator polynomial through the Arnoldi iteration to solve for orthogonal SOS rational functions. This method improves the numerical conditioning to allow approximation of large-order models. Numerical examples have demonstrated the method is able to reliably find rational functions that accurately fit the data, while correcting any possible passivity violations over the entire frequency range of the provided data. Our results demonstrate SOS-based algorithms can consistently provide globally optimal solutions with solving times significantly faster than the direct application of the KYP lemma, and at times comparable to

a known locally optimal passivity enforcement method. The improvements are particularly noticeable for datasets when a large number of frequency samples are used or with increasing number of ports.

REFERENCES

[1] B. Gustavsen and A. Semlyen, "Rational approximation of frequency domain responses by vector fitting," *IEEE Trans. Power Del.*, vol. 14, no. 3, pp. 1052–1061, Jul. 1999.

[2] A. Valera-Rivera and A. E. Engin, "Aaa algorithm for rational transfer function approximation with stable poles," *IEEE Lett. Electromagn. Compat. Pract. Appl.*, vol. 3, no. 3, pp. 92–95, Sep. 2021.

[3] L. E. Carrera-Retana, M. Marin-Sanchez, C. Schuster, and R. Rimolo-Donadio, "Improving accuracy after stability enforcement in the loewner matrix framework," *IEEE Trans. Microw. Theory Techn.*, vol. 70, no. 2, pp. 1037–1047, Feb. 2022.

[4] L. P. R. K. Ihlenfeld and G. H. C. Oliveira, "Completion-based passivity enforcement for multiport networks rational models," *IEEE Trans. Power Del.*, vol. 36, no. 4, pp. 2213–2220, Aug. 2021.

[5] S. Grivet-Talocia, "A perturbation scheme for passivity verification and enforcement of parameterized macromodels," *IEEE Trans. Compon. Packag. Manuf. Technol.*, vol. 7, no. 11, pp. 1869–1881, Jun. 2017.

[6] E. Medina, A. Ramirez, J. Morales, and K. Sheshyekani, "Passivity enforcement of FDNEs via perturbation of singularity test matrix," *IEEE Trans. Power Del.*, vol. 35, no. 4, pp. 1648–1655, Aug. 2020.

[7] T. Bradde, S. Grivet-Talocia, A. Zanco, and G. C. Calafiore, "Data-driven extraction of uniformly stable and passive parameterized macromodels," *IEEE Access*, vol. 10, pp. 15 786–15 804, 2022.

[8] M. Sahouli and A. Dounavis, "Passivity correction of loewner macromodeling using spectral zeros method," in *Proc. IEEE 28th Conf. Elect. Perform. Electron. Packag. Syst.*, 2019, pp. 1–3.

[9] E. M. Aylward, S. M. Itani, and P. A. Parrilo, "Explicit sos decompositions of univariate polynomial matrices and the Kalman-Yakubovich-Popov lemma," in *Proc. 46th IEEE Conf. Decis. Control*, 2007, pp. 5660–5665.

[10] A. Hansson and L. Vandenberghe, "Sampling method for semidefinite programmes with non-negative popov function constraints," *Int. J. Control*, vol. 87, no. 2, pp. 330–345, 2014. [Online]. Available: https://doi.org/10.1080/00207179.2013.833366

[11] Z. Mahmood, B. Bond, T. Moselhy, A. Megretski, and L. Daniel, "Passive reduced order modeling of multiport interconnects via semidefinite programming," in *Proc. Des., Autom. Test Europe Conf. Exhib.*, 2010, pp. 622–625.

[12] P. Benner et al., Eds., *System- and Data-Driven Methods and Algorithms*. Berlin, Germany: De Gruyter, 2021.

[13] A. E. Engin, "Passive scalar function approximation using SOS polynomials," *IEEE Trans. Electromagn. Compat.*, vol. 64, no. 3, pp. 850–855, Jun. 2022.

[14] F. Coronado and A. E. Engin, "Passive modeling of one-port networks through SOS orthogonal rational functions," in *Proc. IEEE Workshop Signal Propag. Interconnects*, Germany, 2022, pp. 1–4.

[15] B. D. O. Anderson and S. Vongpanitlerd, *Network Analysis and Synthesis*. Englewood Cliffs, NJ, USA: Prentice-Hall, Inc., 1974.

[16] C. W. Scherer and C. W. J. Hol, "Matrix sum-of-squares relaxations for robust semi-definite programs," *Math. Prog.*, vol. 107, no. 1–2, pp. 189–211, Jun. 2006.

[17] S. Boyd, L. El Ghaoui, E. Feron, and V. Balakrishnan, *Linear Matrix Inequalities in System and Control Theory.* (SIAM Studies in Applied Mathematics), vol. 15, Philadelphia, PA, USA: SIAM, 1994.

[18] J. Lofberg, "Pre- and post-processing sum-of-squares programs in practice," *IEEE Trans. Autom. Control*, vol. 54, no. 5, pp. 1007–1011, May 2009.

[19] J. Lofberg and P. Parrilo, "From coefficients to samples: A new approach to sos optimization," in *Proc. 43 rd IEEE Conf. Decis. Control*, 2004, vol. 3, pp. 3154–3159.

[20] E. de Klerk, G. Elfadul, and D. den Hertog, "Optimization of univariate functions on bounded intervals by interpolation and semidefinite programming," CentER Discussion paper 2006-26, 2006.

[21] J. M. Hokanson, "Multivariate rational approximation using a stabilized Sanathanan-Koerner iteration," 2020, *arXiv:2009.10803*.

[22] Y. Nakatsukasa, O. Séte, and L. N. Trefethen, "The AAA algorithm for rational approximation," *SIAM J. Sci. Comput.*, vol. 40, no. 3, pp. A1494–A1522, 2018.

[23] C. P. Coelho, J. R. Phillips, and L. M. Silveira, "Generating high-accuracy simulation models using problem-tailored orthogonal polynomials basis," *IEEE Trans. Circuits Syst. I: Regular Papers*, vol. 53, no. 12, pp. 2705–2714, Dec. 2006.

[24] A. Ma and A. E. Engin, "Orthogonal rational approximation of transfer functions for high-frequency circuits," *Int. J. Circuit Theory Appl.*, 2022. [Online]. Available: https://onlinelibrary.wiley.com/doi/pdf/10.1002/cta.3488

[25] A. Semlyen and B. Gustavsen, "A half-size singularity test matrix for fast and reliable passivity assessment of rational models," *IEEE Trans. Power Del.*, vol. 24, no. 1, pp. 345–351, Jan. 2009.

[26] R. Shorten, P. Curran, K. Wulff, and E. Zeheb, "A note on spectral conditions for positive realness of transfer function matrices," *IEEE Trans. Autom. Control*, vol. 53, no. 5, pp. 1258–1261, Jun. 2008.

[27] W. Smith and S. Erdman, "A note on the inversion of complex matrices," *IEEE Trans. Autom. Control*, vol. 19, no. 1, pp. 64–64, Feb. 1974.

[28] N. Wong and Z. Zhang, "Discussion of "A half-size singularity test matrix for fast and reliable passivity assessment of rational models"," *IEEE Trans. Power Del.*, vol. 25, no. 2, pp. 1212–1213, Apr. 2010.

[29] L. Knockaert, F. Ferranti, and T. Dhaene, "Generalized eigenvalue passivity assessment of descriptor systems with applications to symmetric and singular systems," *Int. J. Numer. Modelling: Electron. Netw., Devices Fields*, vol. 26, no. 1, pp. 1–14, 2013.

[30] A. E. Engin, K. Bharath, and M. Swaminathan, "Multilayered finite-difference method (MFDM) for modeling of package and printed circuit board planes," *IEEE Trans. Electromagn. Compat.*, vol. 49, no. 2, pp. 441–447, May 2007.

[31] W. A. Alarcon, A. E. Engin, I. Ndip, and K. Lang, "Ebg common-mode filter design using uncoupled coplanar waveguide to microstrip transitions," *IEEE Lett. Electromagn. Compat. Pract. Appl.*, vol. 2, no. 3, pp. 81–84, Sep. 2020.

[32] B. Gustavsen, "Fast passivity enforcement for s-parameter models by perturbation of residue matrix eigenvalues," *IEEE Trans. Adv. Packag.*, vol. 33, no. 1, pp. 257–265, Feb. 2010.

[33] Sonnet v16.56, [Online]. Available: http://www.sonnetsoftware.com/

[34] M. Grant and S. Boyd, "CVX: Matlab software for disciplined convex programming, version 2.1," Mar. 2014. [Online]. Available: http://cvxr.com/cvx

Francisco Coronado received the B.S. degree in applied physics from California State University, San Marcos, CA, USA, in 2020, and the M.S. degree in electrical engineering from San Diego State University, San Diego, CA, USA, in 2023.

He joined Qualcomm Inc., San Diego, CA, USA, in 2023. His research interests include power and signal integrity.

Arif Ege Engin (Member, IEEE) received the B.S. degree in electrical engineering from Middle East Technical University, Ankara, Turkey, in 1998, the M.S. degree in electrical engineering from the University of Paderborn, Paderborn, Germany, in 2001, and the Ph.D. degree from the Leibniz University Hannover, Hannover, Germany, in 2004.

He was a Research Engineer with the Fraunhofer-Institute for Reliability and Microintegration, Berlin, Germany. From 2006 to 2008, he was an Assistant Research Director with Microsystems Packaging Research Center, Georgia Tech, Atlanta, GA, USA. He is currently a Professor with the Electrical and Computer Engineering Department, San Diego State University, San Diego, CA, USA. He has authored and coauthored more than 100 publications in journals and conferences in the areas of his interests, and five patents. He has coauthored the book *Power Integrity Modeling and Design for Semiconductors and Systems*, translated into Japanese and Chinese (Pearson Education). His research interests include signal and power integrity modeling and simulation.

Dr. Engin was the recipient of the Semiconductor Research Corporation Inventor Recognition Award in 2009, the Outstanding Educator Award from the International Microelectronics Packaging and Assembly Society in 2015, the Alexander-von-Humboldt Research Fellowship for 2015 and 2018, and the 2017 IEEE EMC-S M. Kanda Award for the Most Cited Paper in the last five years (2013–2017).